MEMOIRS OF THE SCHOOL OF ENGINEERING, OKAYAMA UNIVERSITY, Vol. 8, No. 1, JUNE 1973

Effects of Wall Length and Vent on Attaching Jet and Its Switching

Tsutomu WADA*, Akira SHIMIZU*, and Minoru TAKAGI*

(Received May 30, 1973)

Synopsis

The effects of some geometries peculiar to the wall-attachment fluidic devices on the attaching jet flow and the switching mechanism were experimentally made clear. And the propriety of the analytical model, which has been used for the theoretical study of these devices, was investigated.

The results can be summarized as follows:

1) The existing analytical model of the attaching jet flow is not applicable to the case of relatively short wall length of vent distance.

2) The attaching jet flow never detaches from a sufficiently long side wall with vent.

3) The switching mechanism of the vent type device is always the opposite wall switching.

4) From the viewpoint of the output characteristics of the device, the vent distance has a lower limit in relation to the vent width.

1. Introduction

Many studies have been made on the attaching jet flow which is a foundamental phenomenon of the wall attachment fluidic device. Nevertheless, it seems that these results have not been applied well for the design of the device.

For this state, two reasons may be pointed out. Firstly, the attaching jet flow in which the effect of the secondary flow can not

* Department of Industrial Science

be neglected due to the small aspect ratio has not been studied. Secondly, even when the flow may be sufficiently two-dimensional, as pointed out in this paper, it is not yet confirmed well how the specific geometry of device, the wall length, the vent, the splitter, etc., affects the behaviors of the attaching jet flow.

As the authors already reported about the effects of the pointed splitter [1), 2)], the effects of the vent and the attaching wall length are experimentally investigated in this paper.

First, the effects of the vent and the wall length on the jet flow are made clear, and the practical propriety of the results obtained by the model with sufficiently long wall is investigated. Next, the relations between the geometries and the statical switching of the attaching jet flow are made clear in comparison with the ones [3)] of the sufficiently long wall, and the propriety of the analytical model [4)-7)], which has been used for the theoretical study of these devices, is investigated. Beside, Oshima and Matsumoto have recently reported on the effect of the vent on the switching [8)], and the mechanism of some phenomena shown in their paper can be directly explained based on this study.

2. Experimental Setup and Method

In Fig.1 the tested large scale model of the fluidic device is shown. When the splitter is located at sufficiently downstream, it hardly affects the attaching jet flow or the switching mechanism[1),2)],

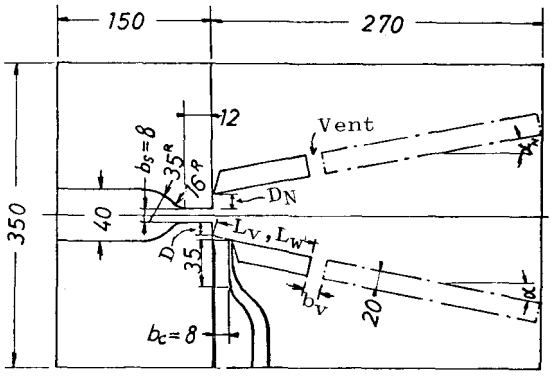

Aspect ratio = 6, $\alpha = \alpha_w = 15^\circ$ (30°)
Control nozzle and side walls are removable, and
these are sealed by petrolatum and clamped by C-clamps.

Fig.1 Large scale model

so it is not used in this model. The jet centerlines (loci of maximum velocity points) and the pressure distributions on the attaching wall were measured by the model with air as the operating fluid. In this case the Reynolds number of the jet Re was 1.3×10^4, using the main nozzle width as the characteristic length.

While, in order to observe the flow patterns and the behavior of jet at the switching, water is used as the operating fluid. Then the flow was visualized by means of the solid tracers, which are the polystyrene granules with 0.5 - 1.0 mm in diameter and the same specific gravity as water[9]. The granules were mixed into the main jet flow by 4 percentages in volume, Re was 9×10^3, and the flow patterns were recorded by a cinecamera.

3. Experimental Results and Discussion

3.1. Effects of Wall Length on Attaching Jet Flow

When the attaching wall is sufficiently long compared with the attachment distance of jet (this case is designated by $L_w/b_s = \infty$), the relations between the control flow rate Q_c/Q_{so} and the attachment distance L_R/b_s are shown by the solid line in Fig.2, where $Q_{so} = \alpha_s b_s \sqrt{2P_s/\rho}$, P_s: supply pressure, α_s: discharge coefficient of main nozzle. On the other hand, when the attaching wall has a finite length, the movement of the attachment point decreases in comparison with the case of the sufficiently long wall, as the control flow rate increases. Then it is guessed that the relation is represented by the chain line in Fig.2, when the control flow rate is increased to the value marked with ● in the figure, the jet detaches from the wall.

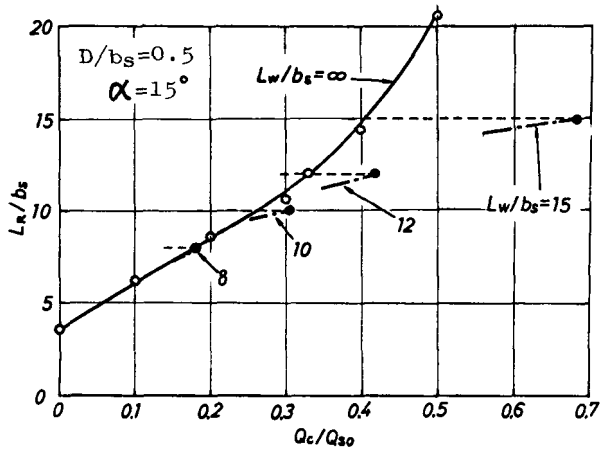

Fig.2 Relations between attachment distance and control flow rate

Here, the discussion is concerned almost only with the experimental results obtained by the model with the offset $D/b_s = 0.5$ and the side wall angle = 15 deg.. However, it is already confirmed that those has generality.

Next, the effects are discussed by the pressure distributions on the attaching wall. In Fig.3, when the value of Q_c/Q_{so} is small, the distributions are same as that in the model with $L_w/b_s = \infty$. Then, it shows that the flow is not yet affected by the wall-end. But, as the value of Q_c/Q_{so} increases further, the mean bubble pressure decreases due to the effects of wall-end*. The distribution for $Q_c/Q_{so} = 0.40$ is shown by the sign ○ in Fig.3. At this time the attachment point must come to the visinity of the wall-end, because the jet detaches from the side wall for $Q_c/Q_{so} = 0.42$. The effect of the wall-end is more remarkable for $L_w/b_s = 15$, but it is hardly recognized for $L_w/b_s = 8$.

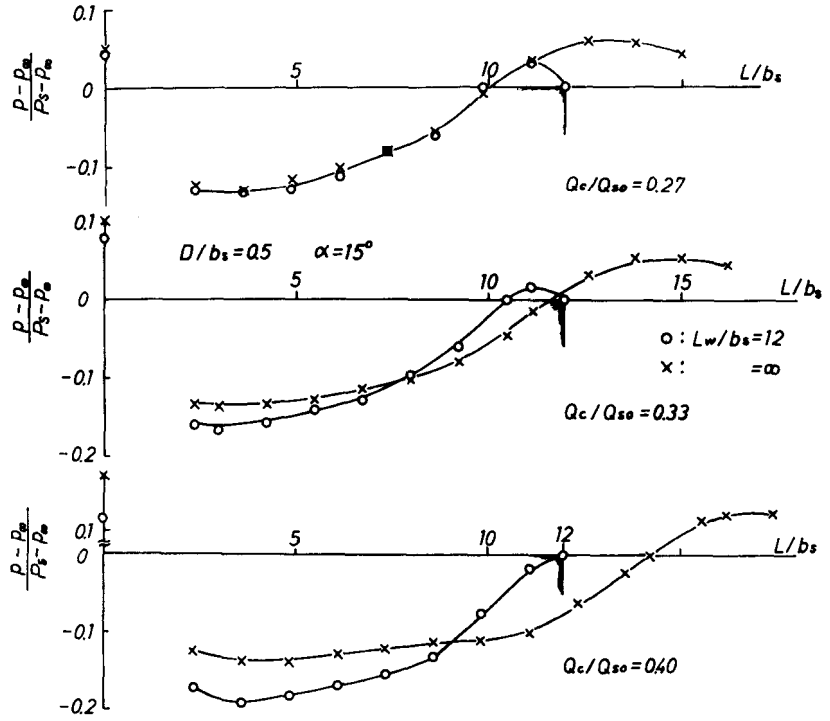

Fig.3 Pressure distributions for finite wall length, compared with that for infinite wall length ($\alpha = 15^\circ$, $D/b_s = 0.5$)

* Bourque and Newman[10] have presented some experimental results and discussions for the effect of wall length on the attaching jet flow without control flow.

As mentioned above, the bubble pressure decreases when the attachment point comes to the visinity of the wall-end. This means that the radious of jet curvature reduces. Some examples are shown in Fig.4, compared with the results for $L_w/b_s = \infty$. In Fig.4 the control flow rates are equal to the rates by which the attachment distances L_R/b_s become 12 and 15 for the model with $L_w/b_s = \infty$, respectively.

And the behaviour of jet is very affected by the existence of the wall-end. This effects can be explained as follows. When the non-dimensional momentum of jet is $\bar{J} = J/J_s$, the momentum of jet flowing downstream from the attachment point $\bar{J}_d = J_d/J_s$, the hypothetical impinging angle against the side wall θ, and the loss of momentum due to to the wall frictional force and the adverse pressure gradient at the vicinity of the attachment point can be neglected, then the radius of curvature of jet R_∞/b_s can be represented by the next formula for $L_w/b_s = \infty$, refering to Fig.5(a),

$$R_\infty/b_s \sim 1/(\bar{J} \cos(\alpha + \delta^*) - \bar{J}_d),$$

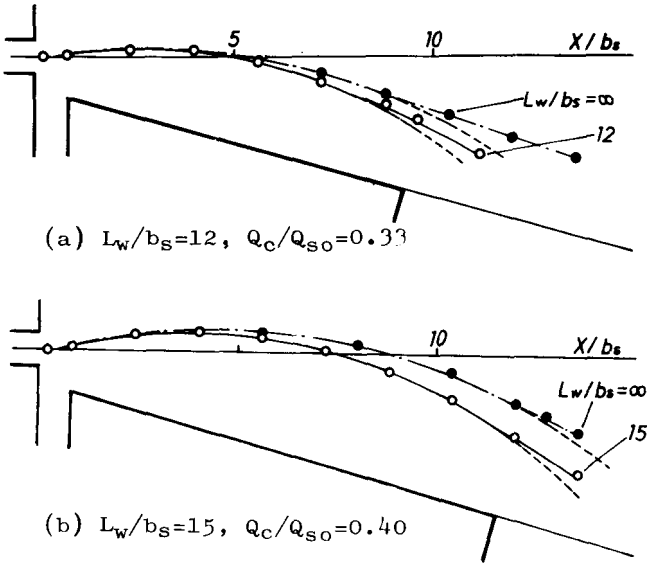

Fig.4 Jet centerlines for finite wall length, compared with that for infinite wall length ($\alpha = 15^\circ$, $D/b_s = 0.5$)

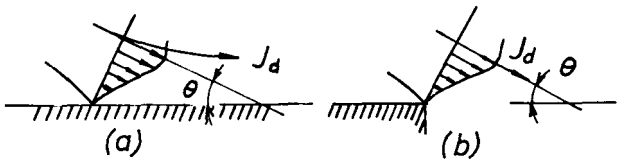

Fig.5 Model of jet

where δ^* is the deflection angle of jet at the upstream section of the control volume.

On the other hand, when the jet is affected by the wall-end, the jet curvature R_{end}/b_s can be represented from Fig.5(b) as follows:

$$R_{end}/b_s \sim 1/(\bar{J} \cos(\alpha + \delta^*) - \bar{J}_d \cos\theta).$$

Therefore, if θ becomes larger, R_{end}/b_s becomes smaller than R_∞/b_s due to the effect of the wall-end. And it can be explained that the negligible effect of the wall-end, such as $L_w/b_s = 8$ in Fig.2, is due to the very small θ.

In Photo.1 the examples of flow patterns are shown to make clear the above phenomena. Here, the model with offset $D/b_s = 2$ is used to observe more clearly the flow near the attachment point. For $Q_c/Q_{so} = 0.3$, two flow patterns of the models with different wall length are almost similar. However, for $Q_c/Q_{so} = 0.45$, those patterns are different due to the effect of the wall-end. Moreover, for $Q_c/Q_{so} = 0.6$, the difference of patterns is remarkable.

The relation between the control flow rate and the attachment distance for the finite wall length is generally different from that for $L_w/b_s = \infty$, as mentioned above. And the degree of effect is very different according to the wall length.

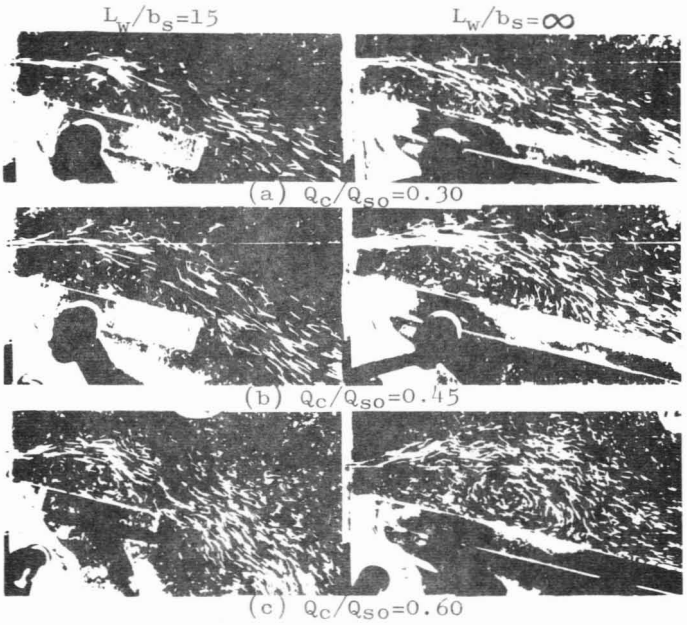

Photo.1 Flow Patterns for short wall length (L_w/b_s=15) and sufficiently long wall (L_w/b_s=∞), in some control flow conditions

3.2. Effects of Vent on Attaching Jet

For the vent with the distance L_v/b_s = 12 and various width and the offset D/b_s = 0.5, the pressure distributions on the side wall are shown in Fig.6. Here, in order to make clear the discussions, the side wall length downstream from the vent is sufficiently large.

For the control flow rate Q_c/Q_{so} = 0.33, the distribution on the wall upstream from the vent is the same as that of L_w/b_s =12 mentioned above. And when Q_c/Q_{so} is further increased to 0.40, the distribution changes only in the case of b_v/b_s = 0.5. This means that the attachment point jumps the vent from the upstream wall to the downstream wall. And then, the attachment bubble grows rapidly due to flow through the vent from the ambient side. For b_v/b_s = 1.5 and 3.0, the attachment point does not yet jump the vent at this control flow rate. For b_v/b_s less than about 3.0, the control flow rate which causes the jump increases with the vent width. For b_v/b_s greater than about 3, this flow rate becomes constant, and this value is equal to the rate of the end wall switching mentioned in later.

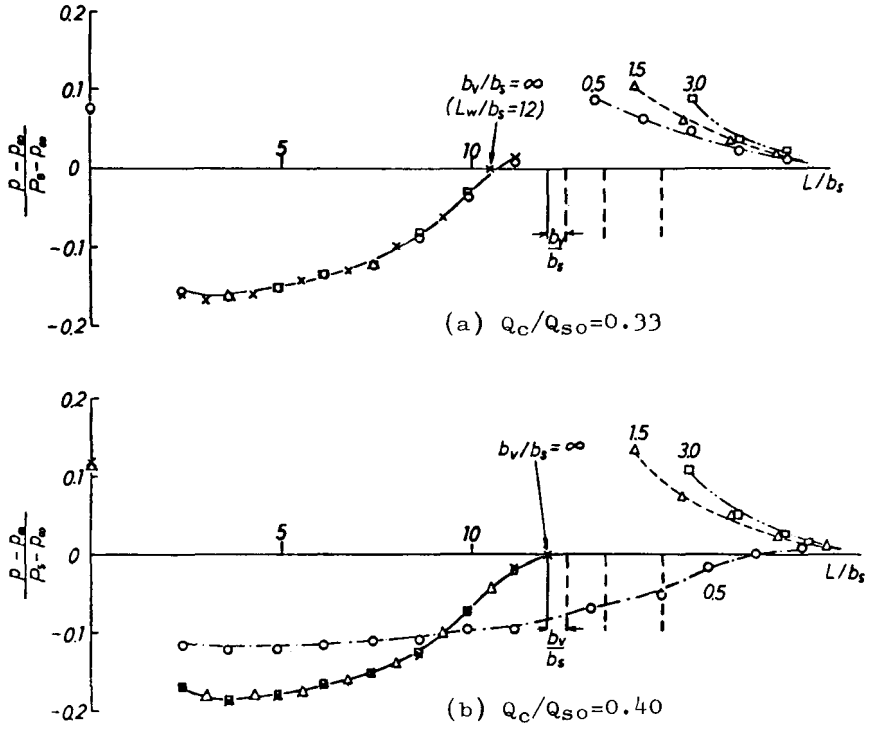

Fig.6 Pressure distributions for various vent conditions (L_v/b_s = 12, D/b_s = 0.5)

The pressure distribution for $L_V/b_S = 8$ is shown in Fig.7. In this case, the control flow rate to cause the jump is independent on the vent width, and is nearly equal to one which detaches the jet from the wall-end. It can be seen that when the impinging angle just before jump is relatively small, as refered in Fig.5(b), the jet is hardly affected by the vent width.

However, after the jump the volume of the attachment bubble directly depends on the vent width.

In Photo.2 some examples of the flow patterns of such case are shown. This indicates clearly that the control flow rate to cause the jump and the attaching bubble volume after jump depend on the vent width.

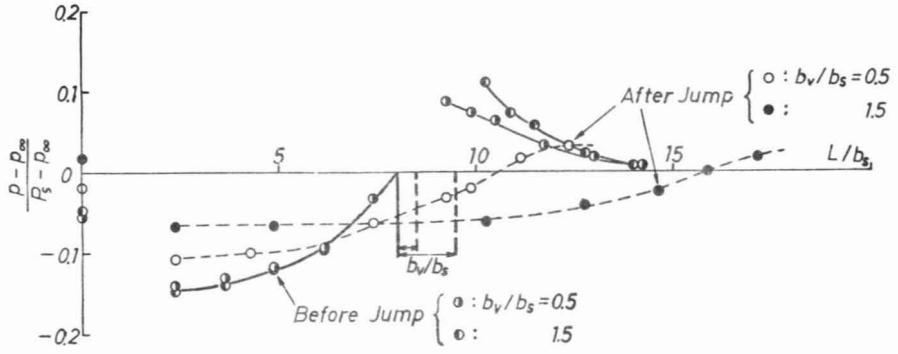

Fig.7 Pressure distributions for some vent conditions ($L_V/b_S = 8$), just before jump of attachment point and after the jump. In this case, the jump is caused by about same control flow rate for all vents.

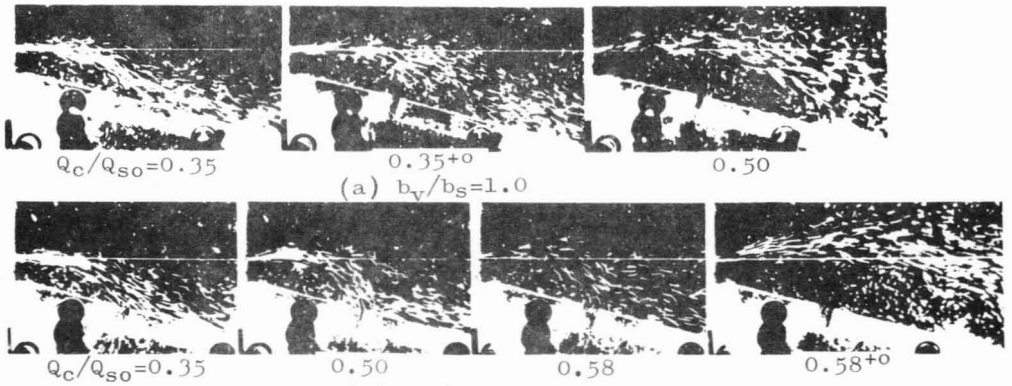

Photo.2 Flow patterns, affected by vent width ($D/b_S = 2$, $L_V/b_S = 12$)

As above mentioned, the jumping phenomenon of the jet occurs for the model with the wall angle greater than 30 deg. Therefore it will be considered that the jet does not detach even after the jump and the weak attaching is kept, if the device has a sufficiently long wall downstream from the vent and the angle α is not so large. The jet behaviour after the jump is dependent on the control flow rate and the entering flow rate into the bubble through the vent.

Thus, if the above two flow rates are introduced in the analysis, the existing analytical method can be applied in this case. More practically, the effects of the splitter on the jet must also be introduced.

3.3. Statical Switching of Attaching Jet

In this section, it is mentioned that how the side wall length and the vent affect the statical switching of the attaching jet. Because of the experiments by means of the model without the splitter, the following discussion does not cover the switching affected by the splitter.

Here, two switching mechanisms are defined as follows: (a) End wall switching.....After the jet detached perfectly from the attaching wall, the jet attaches to the opposite wall, (b) Opposite wall switching.....First, the jet attaches both the walls (i.e. the attaching wall and the opposite wall), and then the initial attachment bubble enlarges and flows away downstream.

Defining in this way, the switching mechanism of the device with the vent belongs to the opposite wall switching, as recognized in the above section. And the end wall switching occurs only in the device with finite wall length.

3.3.1. Effect of Side Wall Length

The relations between the offset of opposite wall D_N/b_s and the control flow rate at switching Q_{cs}/Q_{so} are shown in Fig.8, using the attaching wall length as a parameter. For a constant D_N/b_s, Q_{cs}/Q_{so} decreases in almost whole wall length, as L_w/b_s becomes short. The switching mechanism for these wall lengths is the end wall switching. For the relatively large L_w/b_s, the relations between L_w/b_s and Q_{cs}/Q_{so} are in reverse, and then the switching mechanism is the opposite wall switching.

Such difference of the switching mechanism due to the wall length can be explained as follows. The end wall switching occurs when the attachment point reaches at the wall-end due to the applied control

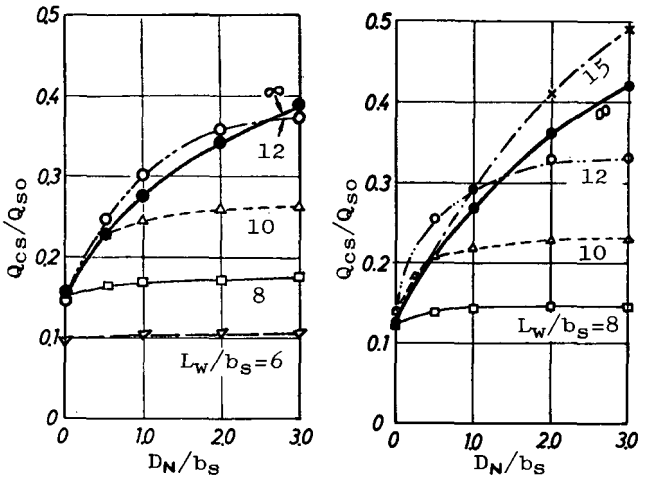

(a) $D/b_s=0.5$ (b) $D/b_s=1.0$

Fig.8 Switching flow rate vs. opposite side wall offset for end wall type devices ($\alpha = \alpha_w = 15°$)

flow rate, and the jet detaches from the wall before attaching to the opposite wall. And as shown in Fig.2, the attachment distance varies with the control flow rate. Therefore, when the end wall switching occurs, Q_{cs}/Q_{so} decreases, as L_w/b_s becomes short. On the other hand, when the opposite wall switching occurs, the above relations are in reverse. As mentioned in section 3.1, when L_w/b_s becomes short, the attachment bubble contracts and this holds down the approach of jet to the opposite wall, thus more control flow rate is required for the opposite wall switching.

In Photo.3 the flow patterns of the switching process are shown for various wall lengths. From these, the difference of two switching mechanisms can be confirmed.

This is one example that the short wall length is in demerit from the standpoint of switching.

In the theoretical analysis of such switching, the effect of the wall-end on the jet flow must be generally considered. However, when the wall length and the offset are not so large, the impinging angle of jet to the attaching wall is not large as mentioned in section 3.1, and then the effect of the wall-end is negligible small.

3.3.2. Effect of Vent

The relations between the opposite wall offset D_N/b_s and the

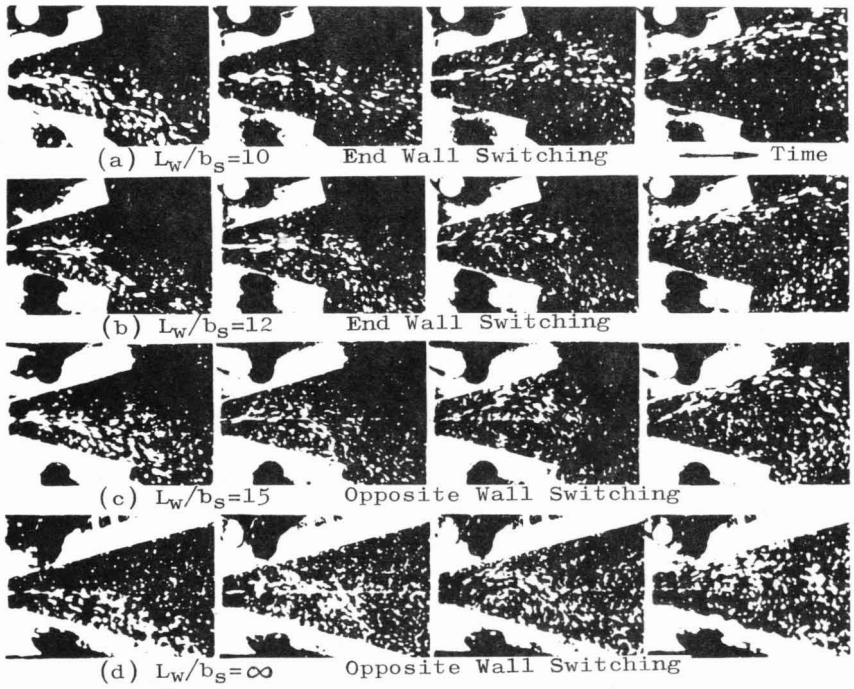

Photo.3 Flow patterns of switching for end wall type devices
(D/b_S = 1.0, D_N/b_S = 1.4)

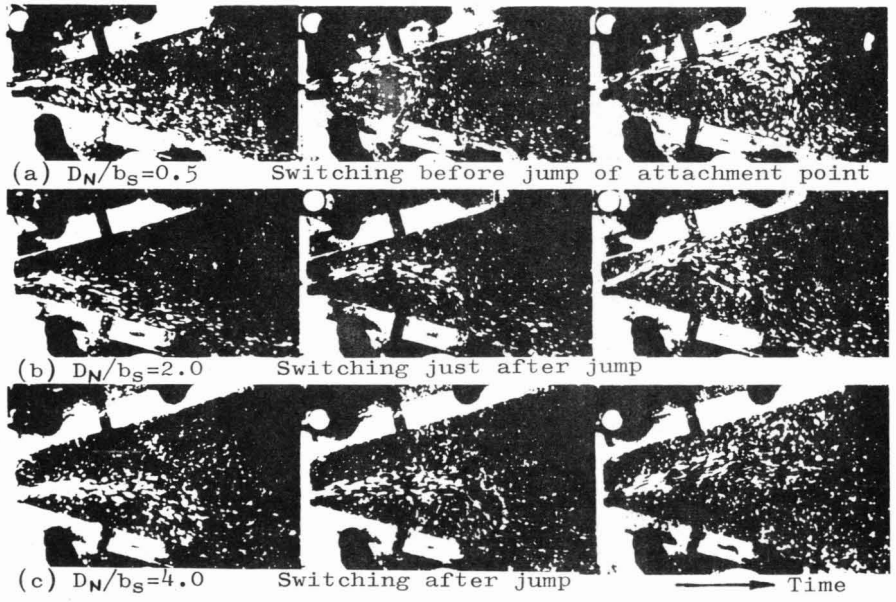

Photo.4 Flow patterns of switching for vent type devices
(D/b_S = 0.5, L_V/b_S = 10, b_V/b_S = 1.5)

switching control flow rate Q_{cs}/Q_{so} for the various vent distances L_v/b_s are shown in Fig.9, using the vent width b_v/b_s as a parameter. The data for the finite wall length ($b_v/b_s = \infty$) and for the attachment wall without the vent ($b_v/b_s = 0$ or $L_w/b_s = \infty$) are shown in the same figure, too.

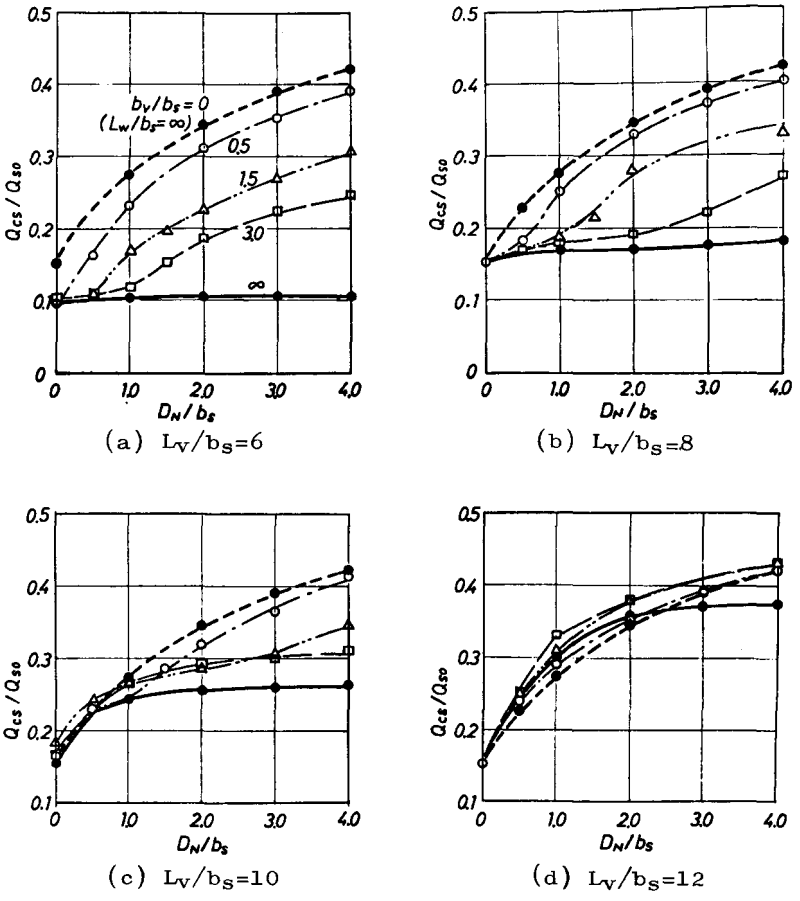

(a) $L_v/b_s=6$ (b) $L_v/b_s=8$

(c) $L_v/b_s=10$ (d) $L_v/b_s=12$

Fig.9 Switching flow rate vs. opposite side wall offset for vent type devices ($D/b_s = 0.5$, $\alpha = \alpha_w = 15^\circ$)

As confirmed from this figure, the switching characteristics of the vent type device is remarkably affected by the vent distance, the vent width, and the offset. The switching modes can be classified into following three: (A) The jet switches before the attachment point jumps over the vent, (B) The jet enters into the switching process at the same time of jumping over the vent, (C) After jumping over the vent, the control flow rate is further required to switch.

And these three switching modes are closely related to the shape of D_N - Q_{cs} curve. First in the mode A, the D_N - Q_{cs} curve is almost independent on b_v/b_s and then has the same tendency as $b_v/b_s = 0$ or $L_w/b_s = \infty$. For example, the region $D_N/b_s < 0.5$ in Fig.9(c) and whole region in Fig.9(d) belong to the mode A.

Next, in the mode B the relation of D_N - Q_{cs} is independent on D_N, but Q_{cs}/Q_{so} increases as b_v/b_s becomes wide. This is shown that the control flow rate required for the jump becomes larger as b_v/b_s becomes wide. For example, the region b_v/b_s = 1.5 to 3.0, and D_N/b_s = 1 to 3 in Fig.9(c) belongs to the mode B.

Moreover, in the mode C, the whole tendency is similar to the case of $b_v/b_s = 0$, and as b_v/b_s becomes narrow, Q_{cs}/Q_{so} becomes larger. This shows that the attachment bubble volume after jumping over the vent is dependent on the flow rate into the bubble through the vent. For example, the region $D_N/b_s > 1$ in Fig.9(a) shows the switching of the mode C.

In Photo.4 the flow patterns of the above three switching modes are shown for $L_v/b_s = 10$, $b_v/b_s = 1.5$. As Q_c/Q_{so} increases step by step, in the case of (a) the switching begins during the attachment point yet exists on the wall upstream from the vent, this is the switching of the mode A. In the case of (b), after the jump of the attachment point over the vent, the attachment bubble volume expands rapidly, and the jet comes near to the opposite wall to enter into the switching process. This is the mode B. In the case of (c), though the bubble volume expands rapidly after the jump, the switching does not yet occur by such Q_c/Q_{so} for large D_N/b_s. Further increasing of the control flow rate causes the switching at last. This is the mode C.

The switching mechanism of the device with vent is substantially the opposite wall switching. Nevertheless, as the effect of vent has not been considered in the existing theories, the interaction between jet and vent must be added to the analytical model of the existing opposite wall switching in order to obtain the more practical model.

3.4. End Wall Switching and its Formation

The switching of an attaching jet flow has mainly investigated in conection with the end wall switching. However, as pointed out in previous section, the end wall switching does not occur for the device with vent. In spite of this statement for the switching, the theory of the end wall switching has practical worth because of the followings.

The usual conditions of the end wall switching are characterized by next two points: (1) the effect of wall-end on the movement of the attachment point is not considered, (2) when the attachment point reaches the wall-end, the switching occurs.

Now, in the case of Fig.9(a) and (b), the condition (1) is approximately satisfied (see Fig.2). And for b_V/b_S = 1.5 and 3.0 and $D_N/b_S < 1$, when the attachment point jumps over the vent, the opposite wall switching just occurs due to the flow into the bubble through the vent. Then, the switching control flow rate is apparently equal to the flow rate by which the attachment point reaches the vent, and the condition (2) is approximately realized.

Therefore, for the device with such geometry, the existing formulation of switching condition is approximately acceptable. This condition is that the jet switches, if and only if the attachment point comes to the wall-end upstream the vent.

3.5. Total Pressure Distribution downstream from Vent under No Load Condition

As mentioned above, the short vent distance is desired from the standpoint of the switching of attaching jet. However, when a part of the jet flow bypasses to the side of ambient pressure through the vent in some cases, the recovery pressure of the device will become smaller.

From this point, the total pressure distributions were measured at a section sufficiently downstream from the vent, when the control flow was not applied. And when the vent distance is a little longer than the attachment distance, the bypass flow through the vent increases remarkably, as the vent width becomes wide.

On the other hand, when the vent distance is longer by $2b_S$ than the attachment distance, the bypass flow is remarkably small.

So, the minimum vent distance which is not disadvantageous on the output characteristics must be larger by $2b_S$ - $3b_S$ than the attachment distance with no control flow. However, when the control nozzle is opened, the minimum vent distance becomes larger than this.

4. Conclusion

The behavior and the switching of attaching jet flow were discussed experimentally by means of the large scale model with the finite wall length and the vent. The results are shown as follows:

(1) For the finite wall length, when the attachment point of jet comes near to the wall-end, the behavior of jet differs from one for the sufficiently long wall. Therefore, in the analysis of this jet, the flow direction downstream from the attachment or anything of the sort must be considered.

(2) When the attachment wall has the vent and the wall length downstream from the vent is sufficiently long, it is recognized that the attachment point jumps over the vent and goes to the wall downstream from the vent for some critical control flow rates. Then, the attaching jet flow never detaches from the wall with vent, though the attachment bubble is opened on the side of ambient pressure through the vent.

(3) When the splitter has no effects on the jet, the switching mechanisms of the attaching jet flow are classified into the end wall switching and the opposite wall switching. The switching mechanism of the vent type device is substantially the opposite wall switching. However, there is the case in which the existing analysis of the end wall switching is apparently proper.

(4) From the standpoint of the switching of jet, the shorter vent distance is desirable, while from the standpoint of the output characteristics of the device, the vent distance has a lower limit in relation to the vent width in order to keep off the bypass flow through the vent under no load condition.

Acknowledgement

The authors wish to thank Dr. H. Hanafusa, proffessor at Kyoto University, for his valuable advice, and to thank Mr. K. Teraoka and Mr. S. Dohta for their assistance in this experiment.

References

1) T. Wada & A. Shimizu: Trans. SICE, 6(1970), 3, 214-220.
2) T. Wada & A. Shimizu: Memoirs of School of Engg., Okayama Univ., 6(1970), 1, 21-25.
3) T. Wada et al.: Proc. of 2nd Internat. JSME Symposium on Fluid Machinary and Fluidics, 3, 171-180 (1972).
4) P.A. Lush: Proc. IFAC Symposium on Fluidics, A3 (1968).
5) H.L. Moses & D.I. McRee: ASME Paper 69-FLCS-31 (1969).

6) M. Kimura: Preprint of IFAC Symposium on Fluidics, A6 (1971).
7) M. Epstein: Trans. ASME, Jour. of Basic Engg., 93(1971), 1, 55-62.
8) Y. Oshima & Y. Matsumoto: Proc. of 2nd Internat. JSME Symposium on Fluid Machinary and Fluidics, 3, 181-190 (1972).
9) E.F. Winter: Progress in Combustion Science and Technology, 1, 1-36, Pergamon Press (1960).
10) C. Bourque & B.G. Newman: Aeronautical Quart., 11(1960), 220-232.